



## Temperature Field in Mass Concrete at Early-Age: Experimental Research and Numerical Simulation

Nguyen-Trong Ho<sup>1</sup>, Trong-Chuc Nguyen<sup>2</sup>, Anh-Kiet Bui<sup>3</sup> and Trong-Phuoc Huynh<sup>4</sup>

<sup>1</sup>Ph.D. candidate, Faculty of Civil Engineering,

VSB Technical University of Ostrava, Ludvika Podesta 1875/17, 708 00 Ostrava-Poruba, Czech Republic.

<sup>2</sup>Lecturer, Le Quy Don Technical University, No. 236, Hoang Quoc Viet St., Hanoi, Vietnam, and Ph.D. candidate, Moscow State University of Civil Engineering, No. 26, Yaroslavskoye Shosse Moscow, Russia.

<sup>3</sup>Lecturer, Ho Chi Minh City Open University,

No. 35 - 37, Ho Hao Hon St., Co Giang Ward, Dist. 1, Ho Chi Minh City, Vietnam.

<sup>4</sup>Lecturer, Department of Civil Engineering, College of Engineering Technology, Can Tho University, Campus II, 3/2 Street, Ninh Kieu District, Can Tho City 900000, Viet Nam.

(Corresponding author: Trong-Phuoc Huynh)

(Received 26 March 2020, Revised 20 May 2020, Accepted 22 May 2020)

(Published by Research Trend, Website: [www.researchtrend.net](http://www.researchtrend.net))

**ABSTRACT:** It is well-known that the hydration of concrete mixture at an early age plays a crucial role in leading to a rise in temperature in massive concrete structures. In addition, thermal stress caused by the temperature difference between the center and the surface of a concrete solid is a crucial reason in making thermal cracking when its stress exceeds the tensile strength of concrete. Therefore, the purpose of this paper is to determine the maximum temperature and the temperature difference in mass concrete with varying scenarios of initial temperature by the use of the finite element Midas Civil code in combination with experimental data. In which, a B30-grade concrete with a water/cement ratio of 0.39 was designed with some temperature sensors for the experimental works. A 3D model mesh of the concrete foundation with 1920 elements and 2509 nodes was used to simulate the scenarios of initial temperature. To verify the accuracy of the finite element simulation results, the simulation results are compared with the measurement results at the construction site. The comparison between the temperature field of simulation with measured temperatures from corresponding sensors was made. It is interesting to found that the difference between the results of measurements and the results of finite element simulation was insignificant. Thus, the finite element method not only gave an accurate prediction of thermal distribution and stress state but also provided a potential indication of cracking ability of concrete at an early age. Furthermore, the analysis results pointed out that the appropriate condition for placing temperature of mass concrete was  $t_{pl} = 30^{\circ}\text{C}$  and also suggested an effective way to control thermal cracking in the mass concrete structure at early-age.

**Keywords:** Hydration heat, Temperature field, Temperature difference, Thermal stress, Mass concrete, Early-age.

**Abbreviations:** FEM, Finite element method.

### I. INTRODUCTION

Mass concrete has been widely used in hydraulic structures, for instance, bridges, dams, spillways, or foundations of high-rise buildings and others. One of the significant factors affecting the stress-strain state of the massive concrete during the construction time and operation process is temperature effect [1]-[3]. The temperature regime in mass concrete structures is affected by many factors, including air temperature, wind speed, the intensity of solar radiation, foundation temperature, and especially the amount of hydration heat caused by the type and content of cement [4].

Besides, the temperature distribution in the mass concrete is also influenced by other factors, for example, the construction schedule, the aggregate size used, the initial temperature of the concrete mix, curing methods, etc. As a result, high-temperature gradient occurring during the construction may cause significant tensile stresses and lead to thermal cracks [5-7]. The temperature differential between the center and the outer surface of the concrete is the reason causing the formation of thermal stress. If the tensile stress is larger than the tensile strength of concrete, thermal cracking

will occur on the surface of the concrete structure.

To avoid the formation of thermal cracks in mass concrete during cement hydration, European ENV 206-1992 standards suggests that the maximum limit of the temperature difference between center and surface should be  $20^{\circ}\text{C}$ . The temperature difference between the center and the surface of a concrete block depends on many factors, for instance, the initial temperature of the concrete mixture, the ambient temperature around the structure, and the thermal properties of the concrete mixture [8].

As a case study, the determination of the maximum temperature and temperature differences in mass concrete of a real building that located in the Ho Chi Minh City of Vietnam with different scenarios of initial temperature is presented in this study with the application of both finite elements Midas Civil code and experimental data. In addition, the comparison between the temperature field obtained from these methods was also made. Moreover, an appropriate value of initial temperature was proposed based on the analysis results in order to control the risk of early-age thermal cracking problems in mass concrete and to be suitable with the real construction conditions.

## II. MATERIALS AND METHODS

### A. Objectives of the research

The building is located in the Ho Chi Minh City of Vietnam, with a total construction area of 232,320 m<sup>2</sup>. The size of the foundation (F12) according to the plan and the thickness of the concrete foundation is 2.5m (Fig. 1). The ambient temperature in the construction area is relatively high, with an average daily temperature of 30°C. The concrete ingredients of the foundation are detailed in Table 1. In which, the designed concrete grade and slump were B30 and 16 ± 2 cm, respectively. A Water-to-cement ratio of 0.39 was used for the mixture. The physical properties of concrete and soil materials are modeled, as shown in Table 2.

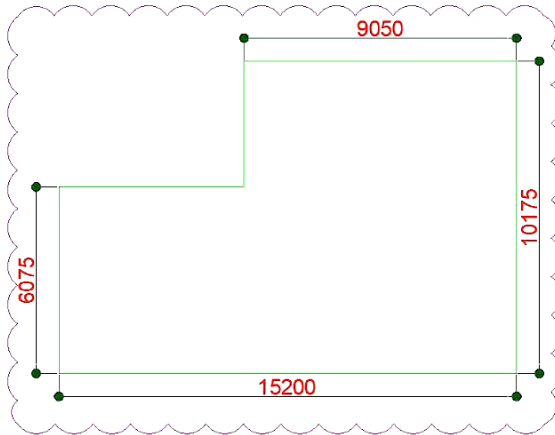


Fig. 1. Plan of foundation F12 (Unit: mm).

Table 1: Mix proportion of concrete.

Materials (kg/m <sup>3</sup> )						
Water	Cement	Fly ash	Sand (0-6) mm	River sand (0-5) mm	Coarse aggregate (5-20) mm	Admixture
160	330	85	359	462	1010	6.4

Table 2: Important parameters of concrete and soil.

Important parameters	Concrete	Soil
Thermal conductivity coefficient, W/(m.°C)	2.9	2.1
Specific heat, kJ/(kg.°C)	1.12	0.85
Specific weight, kg/m <sup>3</sup>	2400	2600
Elastic modulus, N/m <sup>2</sup>	E(t)	1.8×10 <sup>10</sup>
Coefficient of thermal expansion, 1/°C	1×10 <sup>-5</sup>	1×10 <sup>-5</sup>
Poisson's ratio	0.2	0.3
Design compressive strength, MPa	54.41	-

ACI Standard 318-11 shows the relationship of tensile strength and elastic modulus as a function of concrete compressive strength and is presented by equations (1) and (2) [9].

$$f_{sp}(t) = 0.56\sqrt{f'_c} \quad (1)$$

$$E(t) = 4.73\sqrt{f'_c} \quad (2)$$

Where  $f_{sp}(t)$  is the split tensile strength (MPa);  $E(t)$  is Young's modulus (GPa);  $f'_c$  is the compressive strength (MPa).

### B. Analyzing of the heat transfer process in concrete

The solution of the thermal problem is based on the differential equation of the heat conduction theory [10]-[12]:

$$k \left( \frac{\partial^2 T}{\partial x^2} + \frac{\partial^2 T}{\partial y^2} + \frac{\partial^2 T}{\partial z^2} \right) + q_v = \rho c \frac{\partial T}{\partial t} \quad (3)$$

where  $k$  is the thermal conductivity of materials (W/(m°C));  $c$  is specific heat (kJ/(kg.°C));  $q_v$  is the rate of thermal energy generated per unit volume (W/m<sup>3</sup>);  $\rho$  is density (kg/m<sup>3</sup>);  $t$  is the age of concrete at the time (day).

Analysis of heat transfer in mass concrete varies overtime needs to calculate the amount of heat generated heat of cement hydration process, conduction, convection. The main issues when considering heat transfer problems are as follows:

The rate of heat generation of concrete during cement hydration: The increase in heat during cement hydration is determined by equation (4). The magnitude of the heat increase and the shape of the curve can vary and depend on the composition of the concrete mixture [13]-[15]:

$$T(t) = K(1 - e^{-\alpha t}) \quad (4)$$

where  $T(t)$  is the number of heat increases at time  $t$  (°C);  $\alpha$  is the coefficient of temperature rise (reaction rate),  $K$  is the final temperature rise test in adiabatic conditions determined by the equation (5):

$$K = \frac{CQ}{c\rho} \quad (5)$$

where  $C$  is the amount of cement (kg/m<sup>3</sup>);  $Q$  is hydration heat (kJ/kg).

The boundary conditions of the heat transfer analysis problem include the thermal transfer boundary, insulation boundary, and fixed thermal boundary. Because the heat transfer boundary is mainly affected by the concrete surface, the convection model is applied in this model analysis. Convection depends on the type and setting period of the formwork, curing methods of concrete, and wind speed. Newton's law describes the effect of convection as follows [16, 17]:

$$q = hA(T_s - T_a) \quad (6)$$

where  $q$  is heat flow per unit area (kJ/m<sup>2</sup>);  $h$  is convection heat transfer coefficient;  $A$  is area (m<sup>2</sup>);  $T_s$  is the surface temperature (°C);  $T_a$  is air temperature (°C).

The finite element method to solve the problem of heat transfer is expressed by the following equations [18, 19]:

$$[K]\{T\} + [C] \left\{ \frac{\partial T}{\partial t} \right\} = [Q] \quad (7)$$

The time interval for the steps  $\Delta t$  can be described as follows:

$$\left\{ \frac{\partial T}{\partial t} \right\} = \frac{1}{\Delta t} [T(t_n) - T(t_{n-1})] \quad (8)$$

Then, equation (7) can be rewritten as follows:

$$[K]\{T\} + \frac{[C]}{\Delta t} [T(t_n) - T(t_{n-1})] = [Q] \quad (9)$$

where  $K$  is the global stiffness matrix at time  $t_n$ ;  $C$  is a capacity matrix;  $Q$  is a total heat flux vector for internal during hydration and heat convection;  $\Delta t = \Delta t_n - \Delta t_{n-1}$  is steps of computation time.

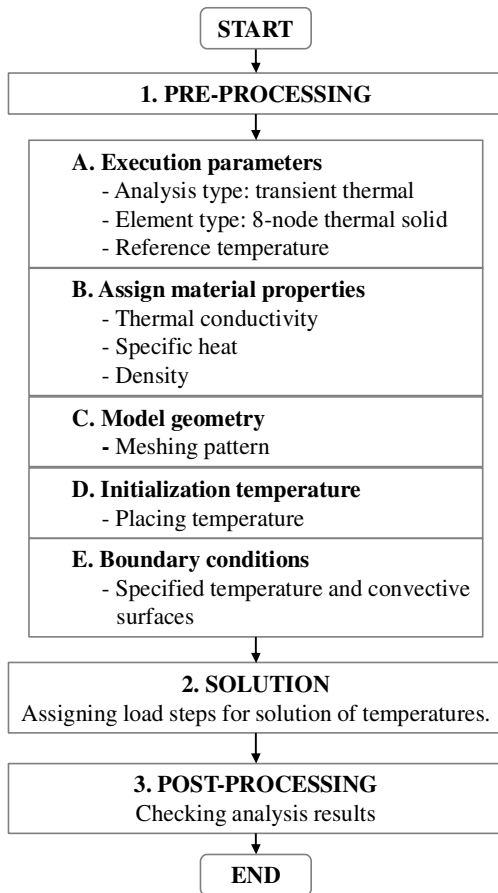


**Fig. 2.** The flowchart of the analysis temperature fields by the finite element method (FEM).

The stiffness matrix is determined by the equation (10):

$$[K] = \int_{\Omega} [B]^T [D] [B] d\Omega \quad (10)$$

where B is the strain-displacement relation matrix; D is the stress-strain relation matrix.

Solving equation (9) allows obtaining temperature fields in concrete mass at different times. The flow diagram of finite element analysis is shown in Fig. 2.

To determine the thermal deformation of a homogeneous, isotropic, elastic body, and equilibrium equations are used [20]:

$$[K]\{u\} + \{f\} = 0 \quad (11)$$

where {u} is the vector of the unknown nodal displacements; {f} is the vector of the nodal loads.

The strain-displacement relation is given by equation (12):

$$\{\varepsilon\} = [B]\{u\} \quad (12)$$

The stress-strain relation is given by equation (13):

$$\{\sigma\} = [D]\{\varepsilon\} \quad (13)$$

where {ε} is the strain matrix; {σ} is the stress matrix.

### III. RESULTS AND DISCUSSION

#### A. Modeling and structural analysis

A 3D model of the concrete foundation is used to simulate the scenarios of initial temperature, as it is shown in Fig. 3. The model mesh is divided into 1920 elements and 2509 nodes.

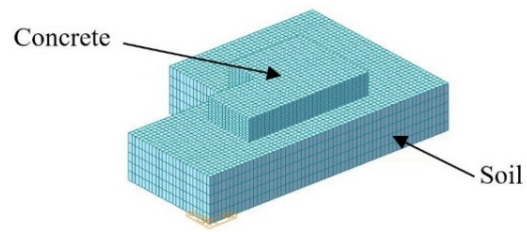


**Fig. 3.** 3D-finite element model mesh of the concrete foundation.

Placing temperature has an important influence on the hydration process of mass concrete at an early age. It is noted that the higher the placing temperature of the concrete mix, the higher the maximum temperature at the center of the concrete block is achieved. The effects of placing the temperature of concrete on the concrete hardening temperatures are shown in Figs. 4 and 5. As can be seen, the maximum temperature at the center of the mass concrete was lower when the placing temperature of concrete varies from 32°C to 25°C. The temperature in the center of the concrete block increases fast and gets the peak values at around 2-3 days after pouring, then the temperature at this location slowly reduces by time. It is found that the maximum temperature at the center of the concrete structure, corresponding to the analysis cases  $t_{pl} = 32^\circ\text{C}$ ,  $30^\circ\text{C}$ ,  $27^\circ\text{C}$ , and  $25^\circ\text{C}$  were  $68.65^\circ\text{C}$ ,  $66.71^\circ\text{C}$ ,  $63.81^\circ\text{C}$ , and  $61.87^\circ\text{C}$ , respectively.

On the other hand, the temperature difference between the center and the surface of mass concrete varies and depends on the initial temperature of the concrete mixture and the ambient temperature. When the initial temperature of a concrete mixture changes from 25°C to 32°C, the temperature difference varies from 17.15°C to 23.73°C. It is worth noting that to prevent the formation of cracks, the temperature difference between the inside (center) and the surface does not exceed 20°C. From Fig. 5, it can be seen that the temperature difference with the cases of placing temperature ( $t_{pl} = 25^\circ\text{C}$ ,  $27^\circ\text{C}$ , and  $30^\circ\text{C}$ ), the temperature difference was smaller than the allowed temperature difference. Thus, to reduce construction costs, the initial temperature was chosen to be 30°C.

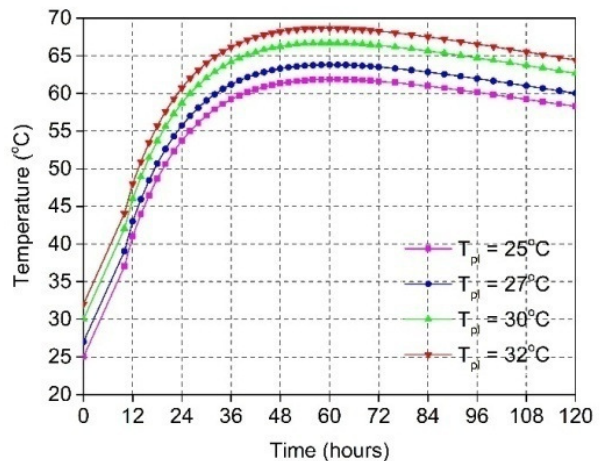


**Fig.4.** Temperature development at the center in mass concrete.

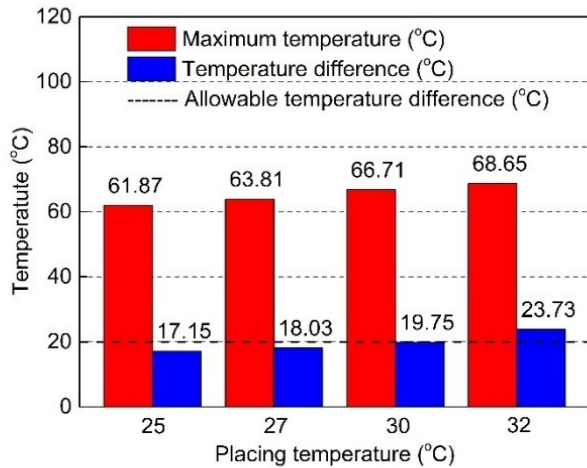


**Fig. 5.** The relation between placing temperature and the maximum temperature, the temperature drop in the concrete foundation.

*B. Verify the results of the finite element method with field measurements*

To verify the accuracy of the finite element simulation results, the simulation results are compared with the measurement results at the construction site. The locations of the temperature sensors put on the foundation block are pointed out in Fig. 6. Sensors B1, C1, and T1 were placed along the vertical centerline of the foundation. And sensors B2, C2, and T2 were placed 0.4 m from the corner of the foundation. The temperature of locations in the foundation measured from the sensors is shown in Figs. 7 and 8. Additionally, the comparison between the temperature field changes over time of simulation with measured temperatures corresponding sensors is presented in Figs. 7 and 8.

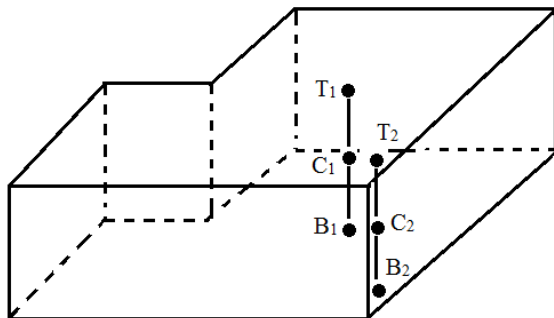
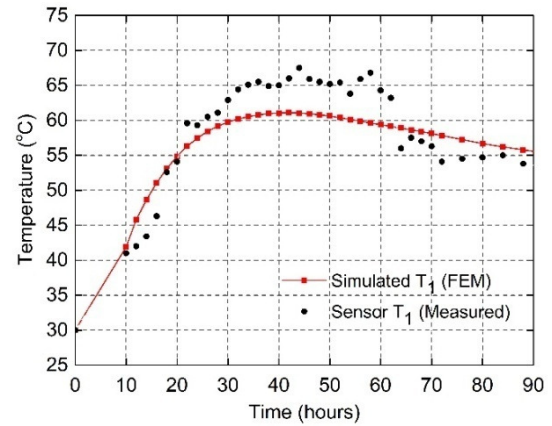
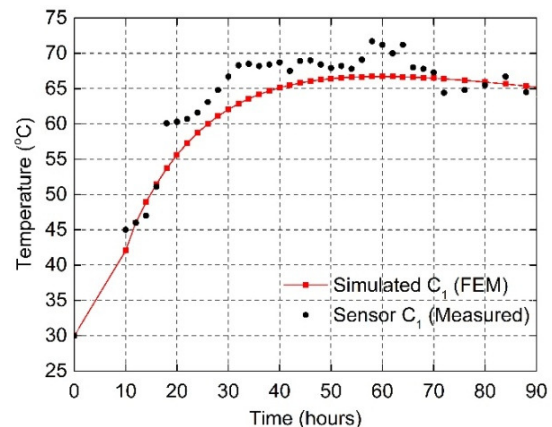


**Fig. 6.** The locations put on the temperature sensor in the foundation.

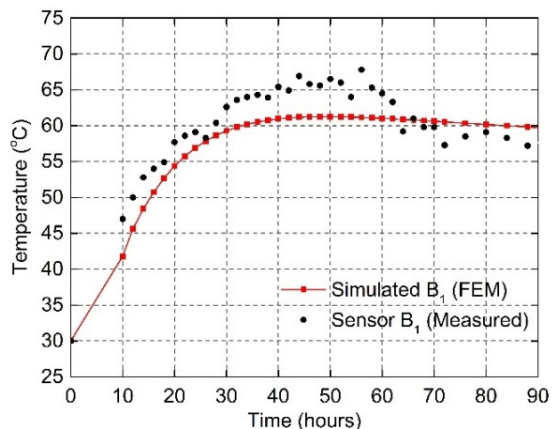
The trend of temperature development from the obtained FEM model is relatively close to the development trend of temperature obtained from sensors (data collected from site measurement). The temperature value from the calculation model is close to the measured temperature value at the construction site. However, the temperature field from the model results is lower than the temperature field obtained from the measurement. The difference is related to influencing factors, for example, solar radiation, atmospheric radiation, or changes in environmental temperature that the model calculation did not take into account.



(a)



(b)



(c)

**Fig. 7.** Simulated and measured temperatures at the center of the foundation for sensors.

Fig. 9 shows the temperature distribution in the foundation after 60 hours of concrete placement in a 3D cut-off view at the center a) and the corner b) of concrete foundation. Due to faster heat dissipation on the concrete foundation, the temperature distribution on the cross-section at the corner of the concrete foundation is lower than the temperature distribution in the center of the concrete foundation at the same time.

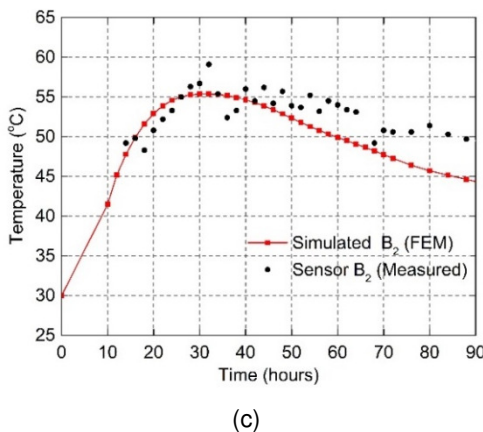
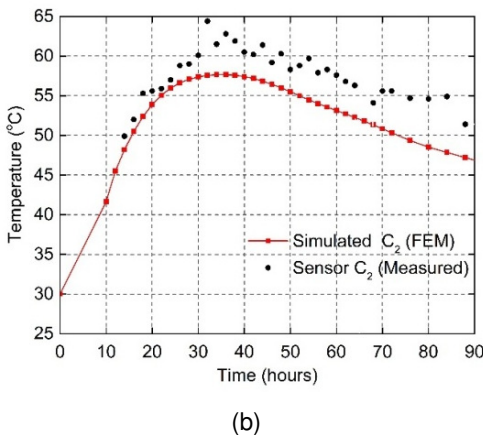
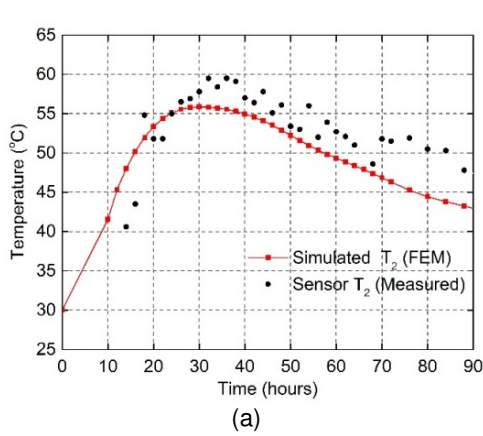


**Fig. 8.** Simulated and measured temperatures at the corner of the foundation for sensors.

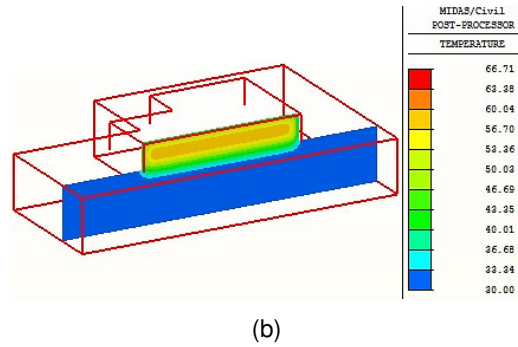
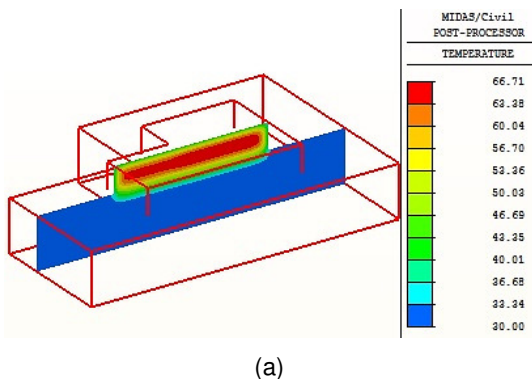


**Fig. 9.** The temperature field of the foundation (a) at the center and (b) at the corner after 60 hours of concrete placement.

Fig. 10 shows the thermal stress development of the six points (as it is shown in Fig. 6) in the concrete foundation. During the hydration of cement, the volume of the concrete foundation expanded and contracted during cooling. However, the center temperature is always higher than the surface or near-surface temperature, which creates a temperature difference between the center and the surface of the concrete foundation. Therefore, during increasing temperature, the volume expansion inside the center is more significant than the surface. So, the compressive stress appears in the center, and tensile stress appears near the surface or surface. This tensile stress can cause crack formation if the tensile stress value exceeds the allowable tensile stress value. Fig. 10 shows that all points for thermal stress surveys are always smaller than the allowable tensile stress value. Therefore, no cracks are formed in the concrete foundation.

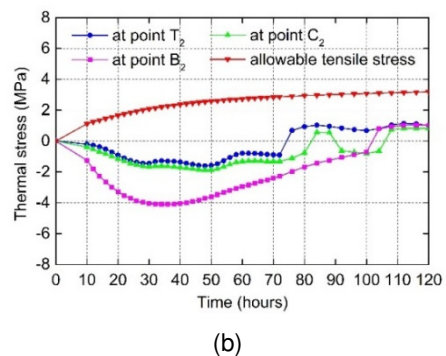
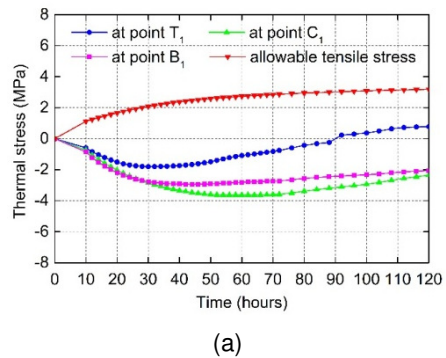


**Fig. 10.** The stress development (a) at the center (T1, C1, B1) and (b) at the corner (T2, C2, B2) of the concrete foundation.

#### IV. CONCLUSION

From the research results obtained, give the following conclusions: *First*, the results from measurements and the results from finite elements show that the difference is not significant. So, the finite element method can give an accurate prediction of thermal distribution, stress state as well as provide a potential indication of cracking ability of concrete at an early age. *Second*, based on the selected concrete mix proportion, the higher the placing temperature causes the higher the maximum temperature in the center of the concrete block. When the placing temperature is 30°C, the maximum temperature difference between the center and the surface of the concrete block does not exceed the limits to avoid the thermal cracks. *Third*, this paper presents the causes and characteristics of cracking of mass concrete at an early age briefly. Besides, the initial temperature of the concrete mixture was reviewed and selected to avoid causing cracking at an early age. The discussed problems will be further investigated in the next papers that will be focused on the influence of structural, materials, and technological factors on the development of temperature, moisture, and finally induced stresses.

#### V. FUTURE SCOPE

The large scale of site measurements could be performed in order to increase the accuracy of the results.

**Conflict of Interest:** The authors declare that there is no conflict of interest regarding the publication of this paper.

#### REFERENCES

- [1]. ACI 207.1R-05. *Guide to Mass Concrete*. Reported by ACI Committee 207, 2012.
- [2]. Klemczak, B., Batog, M., Pilch, M. and Žmij, A. (2017). Analysis of Cracking Risk in Early Age Mass Concrete with Different Aggregate Types. *Procedia Engineering*, 193: 234–241.
- [3]. Aniskin, N., Nguyen, T. C. and Hoang, Q. L. (2018). Influence of Size and Construction Schedule of Massive Concrete Structures on Its Temperature Regime. *MATEC Web of Conferences*, 251: 02014.
- [4]. Krejčí, T., Koudelka, T. and Kruis, J. (2015). Numerical Modeling of Coupled Hydrothermo-Mechanical Behavior of Concrete Structures. *Pollack Periodica*, 10(1): 19–30.
- [5]. Klemczak, B. and Knoppik-Wróbel, A. (2011). Early Age Thermal and Shrinkage Cracks in Concrete Structures– Description of the Problem. *Architecture Civil Engineering Environment*, 2: 35–48.
- [6]. Fall, Y., Chourak, M., Cherif, S. E., Himi, M. and Rougui, M. (2019). Influence of Gravel and Adjuvant on the Compressive Strength and Water Absorption of Concrete. *Pollack Periodica*, 14(1): 95–106.
- [7]. Tang, V. L., Nguyen, T. C., Bulgakov, B. I. and Pham, N. A. (2018). Composition Calculation and

- Cracking Estimation of Concrete at Early Ages. *Magazine of Civil Engineering*, 82(6): 136–148.
- [8]. Aniskin, N. A., Nguyen, T. C., Bryansky, I. A. and Dam, H. H. (2018). Determination of the Temperature Field and Thermal Stress State of the Massive of Stacked Concrete by Finite Element Method. *Vestnik*, 13(11): 1407–1418.
  - [9]. ACI 318-11. *Building Code Requirements for Structural Concrete*. American Concrete Institute, 2011.
  - [10]. Do, T. A., Lawrence, A. M., Tia, M. and Bergin, M. J. (2013). Importance of Insulation at the Bottom of Mass Concrete Placed on Soil with High Groundwater. *Transportation Research Record: Journal of the Transportation Research Board*, 2342(1): 113–120.
  - [11]. Lawrence, A. M. *A Finite Element Model for the Prediction of Thermal Stresses in Mass Concrete*. Ph.D. Thesis, University of Florida, USA, 2009.
  - [12]. Aniskin, N. A. and Nguyen, T. C. (2018). The Thermal Stress of Roller-Compacted Concrete Dams During Construction. *MATEC Web of Conferences*, 196: 04059.
  - [13]. Nguyen, T. C., Tang, V. L. and Bulgakov, B. I. (2018). Designing the Composition of Concrete with Mineral Additives and Assessment of the Possibility of Cracking in Cement Concrete Pavement. *Material Science Forum*, 931: 667–673.
  - [14]. Havlásek, P., Šmilauer, V., Hájková, K. and Baquerizo, L. (2017). Thermo-Mechanical Simulations of Early-age Concrete Cracking with Durability Predictions. *IOP Conference Series, Materials Science and Engineering*, 236: 32–40.
  - [15]. Rahimi, A. and Noorzai, J. (2011). Thermal and Structural Analysis of Roller Compacted Concrete (R.C.C) Dams by Finite Element Code. *Australian Journal of Basic and Applied Science*, 5(12): 2761–2767.
  - [16]. Noorzai, J., Bayagoob, K. H., Abdulrazeg, A. A., Jaafar, M. S. and Mohammed, T. A. (2009). Three Dimensional Nonlinear Temperature and Structural Analysis of Roller Compacted Concrete Dam. *Engineering*, 47(1): 43–60.
  - [17]. Nguyen, T. C., Huynh, T. P. and Tang, V. L. (2019). Prevention of Crack Formation in Massive Concrete at an Early Age by Cooling Pipe System. *Asian Journal of Civil Engineering*, 20(8): 1101–1107.
  - [18]. Xu, Y., Xu, Q., Chen, S. H. and Li, X. X. (2017). Self-Restraint Thermal Stress in Early-Age Concrete Samples and Its Evaluation. *Construction and Building Materials*, 134: 104–115.
  - [19]. Zhu, B. F. *Thermal Stresses and Temperature Control of Mass Concrete*. Butterworth-Heinemann, Waltham, 2014.
  - [20]. Kuzmanovic, V., Savic, L. and Mladenovic, N. (2013). Computation of Thermal-Stresses and Contraction Joint Distance of RCC Dams. *Journal of Thermal Stresses*, 36(2): 112–134.

**How to cite this article:** Nguyen-Trong Ho, Trong-Chuc Nguyen, Anh-Kiet Bui and Trong-Phuoc Huynh (2020). Temperature Field in Mass Concrete at Early-Age: Experimental Research and Numerical Simulation. *International Journal on Emerging Technologies*, 11(3): 936–941.